Published in final edited form as:

Nature. 2012 August 16; 488(7411): 399–403. doi:10.1038/nature11248.

Slings enable neutrophil rolling at high shear

Prithu Sundd[1], **Edgar Gutierrez**[2], **Ekaterina K. Koltsova**[1], **Yoshihiro Kuwano**[1,3], **Satoru Fukuda**[3], **Maria K. Pospieszalska**[1], **Alexander Groisman**[2], and **Klaus Ley**[1,*]

[1]Division of Inflammation Biology, La Jolla Institute for Allergy and Immunology, La Jolla, CA, 92037

[2]Department of Physics, University of California San Diego, La Jolla, CA, 92093

[3]Laboratory of Electron Microscopy, University of Tokyo, Tokyo, Japan

Abstract

Most leukocytes can roll along the walls of venules at low shear stress (1 dyn/cm^2), but neutrophils have the ability to roll at 10-fold higher shear stress in microvessels *in vivo*[1,2]. The mechanisms involved in this shear-resistant rolling are known to involve cell flattening[3] and pulling of long membrane tethers at the rear[4–6]. Here, we show that these long tethers do not retract as postulated[6,7], but instead persist and appear as 'slings' at the front of rolling cells. We demonstrate slings in a model of acute inflammation *in vivo* and on P-selectin *in vitro*, where P-selectin-glycoprotein-ligand-1 (PSGL-1) is presented as discrete sticky patches while LFA-1 is expressed over the entire length on slings. As neutrophils roll forward, slings wrap around the rolling cells and undergo a step-wise peeling from the P-selectin substrate enabled by the failure of PSGL-1 patches under hydrodynamic forces. The 'step-wise peeling of slings' is distinct from the 'pulling of tethers' reported previously[4–6,8]. Each sling effectively lays out a cell-autonomous adhesive substrate in front of neutrophils rolling at high shear stress during inflammation.

Neutrophil rolling at high shear stress is poorly understood[2]. Some neutrophil adhesion molecules including PSGL-1 are concentrated around the tips of microvilli, where they initiate contact with the vessel wall[9,10]. When the force on a microvillus exceeds a threshold force of ~31 pN, the plasma membrane eventually separates from the cytoskeleton, forming a tether[8,11]. To study the footprints of cells rolling under high shear, we recently developed quantitative Dynamic Footprinting (qDF)[4] and refined it to allow simultaneous acquisition of two fluorochromes (DqDF)[12]. qDF relies on total internal reflection fluorescence (TIRF)

Corresponding author: Klaus Ley, M.D., Head Division of Inflammation Biology, La Jolla Institute for Allergy & Immunology, 9420 Athena Circle Drive, La Jolla, CA 92037., (858) 752–6661 (tel), (858) 752–6986 (fax), klaus@liai.org.

Supplementary Information is linked to the online version of the paper at www.nature.com/nature.

Author contributions. P.S. performed all the experiments and image analysis. E.G. and A.G. designed the microfluidic device. M.K.P. calculated the fraction of bond force and torque shared by slings and tethers. E.K.K. was involved in culturing of Th1 CD4T cells. Y.K. and S.F performed the scanning electron microscopy. P.S. and K.L. wrote the manuscript. K.L. supervised the project. All authors discussed the results and commented on the manuscript.

Author information. Reprints and permissions information is available at www.nature.com/reprints.

Authors have no competing financial interests.

microscopy of fluorescent neutrophils rolling in microfluidic channels on glass substrates coated with P-selectin. We observed that DiI-stained neutrophils isolated from the bone marrow of WT mice (Fig. 1a and Supplementary movie 1) or neutrophils in whole blood of *Lyz2-EGFP* mice[13] (Fig. 1b and Supplementary movie 2) rolling at 6–10 dyn/cm^2 frequently formed long processes in the downstream direction. These structures have not been observed previously, and we propose to call them “slings”. 3D-reconstructions of the qDF footprint of a rolling neutrophil with a sling in front is shown in Figures 1c–d (Supplementary note 1). Scanning electron micrographs (SEMs; Fig. 1e) confirm that neutrophils rolling at 10 dyn/cm^2 have slings in front and tethers in the rear. As the cells roll forward, the slings are wrapped around the rolling neutrophils, which was revealed both by qDF (Fig. 1f and Supplementary movie 3) and SEMs (Fig. 1g).

Slings were observed *in vivo* by epifluorescence intravital microscopy of mouse cremaster venules. Slings in front of six different leukocytes (labeled with a mAb against LFA-1) rolling in cremaster venules of WT mice *in vivo* are shown in Figure 1h–m, Supplementary figure 1, and Supplementary movies 4 and 5.

When a neutrophil is first captured from the flow, an initial sling may take several seconds to form. Slings become more frequent as the rolling progresses at high shear stress (Fig. 2a–b) and their average length increases with shear stress over the range of 6 to 10 dyn/cm^2 (Fig. 2c; Supplementary note 2). Since neutrophil rolling at high shear stress produces 3–4 tethers per cell[4], we hypothesized that slings may form when detached tethers swing around to the front of the rolling cell. This was confirmed by both qDF (Fig. 2d and Supplementary movie 6) and DIC microscopy (Fig. 2e and Supplementary movie 7). Since each tether grows over time, and the aspect ratio of the tether anchorage points suggested increasing force (Supplementary fig. 2), we calculated the tether force based on the nonlinearly decaying spring viscoelasitic (NLDs-viscoelastic) model[8]. Although the anchorage points along newly formed slings initially did not show evidence of deformation, this changed as the cell rolled over the sling, which resulted in the rearmost patch to become load-bearing (white arrowhead at t = 13 s in Fig. 1a and t = 5 s in Fig. 1b). The force acting on a tether or a load-bearing sling reached a maximum of 80–90 pN just before the tether or sling detached (Fig. 2f). If a rolling cell has two loaded slings and two tethers with the inflection points (white arrowhead at t = 13 s in Fig. 1a) and anchorage points (white arrowhead in Supplementary Fig. 2a), respectively, at a distance of 10 μm from the cell center, then the 2 slings and 2 tethers can together balance the entire bond torque and more than ¾ of the forward force acting on the rolling cell (Fig. 2g and Supplementary fig. 3). Thus, tethers and slings are the major structures which slow down neutrophils rolling at high wall shear stress.

qDF experiments with both naïve and Th1 CD4T cells (Supplementary note 3; Supplementary fig. 4 and 5) revealed that the formation of slings is indeed associated with stabilized rolling at high shear stress. Next, we addressed the nature of PSGL-1 expression on slings. Raw DqDF images of WT neutrophils rolling on P-selectin (Supplementary fig. 6a) show the expression of PSGL-1 (4RB12 mAb[14]; green) on the cell surface, sling, and tether anchorage points. Consistent with previous results in suspended cells[9,10], PSGL-1 is localized around the tips of microvilli of rolling neutrophils (Supplementary fig. 6b), but excluded from the cell surface. As anticipated, PSGL-1 (green) was present in the tether

anchorage points, but surprisingly, PSGL-1 (green) was also expressed in patches along the sling. Further experiments were conducted using a red fluorochrome (Alexa-Fluor-568) coupled to 4RB12 mAb (Fig. 3a–c and Supplementary fig. 7 and 8). Specificity was established by investigating PSGL-1-deficient neutrophils rolling on E-selectin which showed no staining for PSGL-1 (Supplementary fig. 9). We observed a high concentration of PSGL-1 not only at the tip (the former tether anchorage point), but also in discrete patches along the length of slings (Fig. 3a and Supplementary fig. 7 and 8). Analysis of SEM images of slings revealed tips of microvilli preserved as lobes on the slings (Supplementary fig. 10 and 11). These findings suggest that membrane from several microvilli is pulled from the cell surface to form the tethers. Tethers following detachment become slings and the tips of microvilli which are rich in PSGL-1 appear as patches on the slings. Indeed, the spacing of PSGL-1 patches on slings (1.6 ± 0.2 (s.e.m.) μm; $n = 34$) is comparable to the estimated distance between the tips of adjacent microvilli (1.32 μm) preserved as lobes on a 10 μm long sling (Supplementary fig. 12).

As each sling wraps around the rolling cell, each of the PSGL-1 patches functions as a discrete point of attachment with the P-selectin substrate (Fig. 3c, Supplementary fig. 13, and Supplementary movie 8). When a PSGL-1 patch on the sling becomes load-bearing, the bond force pulls the patch away from the substrate in the *z*-direction (Figure 3d and Supplementary figure 14). Concomitantly, the apparent brightness of a PSGL-1 patch decreases by 50–75% (Fig. 3e and Supplementary fig. 15) as the bonds get loaded because the intensity of the TIRF evanescent wave exponentially decreases with *z*-distance from the cover slip[4]. On tethers, PSGL-1 is concentrated in the tether anchorage point (Fig. 3b). When the PSGL-1 patch at the tether anchor point breaks, this results in catastrophic failure (step 1 in Fig. 3f), because there is no chance that the bonds can re-form. However, on slings, PSGL-1 is organized in patches and unlike a tether, a sling peels in a step-wise manner (Fig. 3c, f and Supplementary fig. 13). Figure 3g shows the impact of the failure of sling patches and tethers on the forward displacement of the cell shown in Figure 3c. When a patch of PSGL-1 bonds fails, the sling is pulled taught by the rolling neutrophil until the next PSGL-1 patch becomes loaded. As a consequence, the forward displacement of the rolling cell following a patch failure is smaller (0.2 ± 0.1 (s.d.) μm; $n = 2$; Fig. 3g) than that of a tether failure (1 ± 0.3 (s.d) μm; $n = 4$; Fig. 3g), and the increase in displacement is short lived because a new bond patch is available to be loaded within less than 2 μm. The complete loss of a sling (between 2.2 and 2.4 s in Fig. 3g) is equivalent to the breaking of a tether, which results in a large forward displacement, because no new PSGL-1 patch is available to bear the load. A similar analysis of two more cells (Supplementary fig. 16 and 17) show that the slings indeed act as breaks on rolling neutrophils. This was further corroborated by the *in vivo* observation (Supplementary fig. 18) that rolling leukocytes slow down following sling formation in cremaster venules of mice. ‘Step-wise peeling of slings’ (white thin arrow in Supplementary fig. 19) is distinct from ‘pulling of tethers’[4,5] (white arrowhead in Supplementary fig. 19). The two mechanisms probably work synergistically to facilitate shear-resistant rolling.

Under inflammatory conditions *in vivo*, mouse $\alpha_L\beta_2$-integrin LFA-1 binds ICAM-1[15] and ICAM-2[16] and is known to be responsible for neutrophil slow rolling[17] and arrest[18]. Unlike

PSGL-1, LFA-1 is uniformly expressed on the surface of WT (Fig. 4a–b, Supplementary fig. 20, 21, and Supplementary movie 9) but not LFA-1 deficient neutrophils (Supplementary fig. 22) and colocalizes with the footprint, tether anchorage points and slings (Fig. 4c). To directly show the differential distribution of PSGL-1 and LFA-1, we labeled the same cell suspension with both non-blocking-anti-PSGL-1 (red or green) and anti-LFA-1 (green or red) mAbs. Again, LFA-1 was seen in the footprint, tether anchorage points and slings, while PSGL-1 was restricted to microvilli tips, tether anchorage points and spots on slings (Fig. 4b and Supplementary fig. 23 and 24).

We have previously shown that neutrophils rolling on P-selectin acquire some LFA-1 in the extended conformation with intermediate affinity that can bind to ICAM-1 on the substrate to support a rolling interaction[17,19]. As slings are rich in LFA-1 and wrap around rolling neutrophils, we investigated whether slings can mediate LFA-1-ICAM-1 or LFA-1-ICAM-2 interactions in *trans* in rolling neutrophils. A recent study has shown that ICAM-1 is upregulated on a subset of mouse whole blood neutrophils during ischemia-reperfusion injury[20]. Flow cytometry (Supplementary fig. 25a–c) showed that ICAM-1 is absent on blood and minimally expressed on bone marrow mouse neutrophils under the conditions used in this study. However, ICAM-2 was abundantly expressed on bone marrow neutrophils (Supplementary fig. 25d–f). Bone marrow neutrophils from WT or LFA-1 deficient (*Itgal*$^{-/-}$) mice either untreated or blocked with function blocking Abs against LFA-1[17] or ICAM-2[21] were allowed to roll on P-selectin and the rolling velocities were compared (Fig. 4d). To our initial surprise, absence of LFA-1 or blocking LFA-1 or ICAM-2 resulted in a small but reproducible decrease in rolling velocity (Fig. 4d). As a positive control, bone marrow neutrophils from WT mice were also allowed to roll on glass substrate coated with both P-selectin and ICAM-1. This resulted in much larger decrease in rolling velocity (Supplementary fig. 26) as shown previously[19]. As expected, treatment with function blocking anti-LFA-1 mAb returned the rolling velocity to the level seen with LFA-1 blockade on a P-selectin substrate, but not to the higher level seen in neutrophils rolling on P-selectin without blockade of LFA-1 or ICAM-2 (Supplementary fig. 26). DqDF images (Fig. 4e and Supplementary fig. 27) show that although LFA-1 (red) is expressed both on cell surface and slings, ICAM-2 (green) is expressed mostly on the cell surface. These data suggest that the LFA-1 on slings interacts with ICAM-2 on the cell surface in *trans*. Green staining was absent in neutrophils stained with Alexa-Fluor-488-conjugated Rat $IgG_{2a\kappa}$ (green) Ab (Supplementary fig. 28). LFA-1 binding to ICAM-2 is expected to cause the sling to be more tightly wrapped around the rolling neutrophil, thus creating a less favorable lever arm (distance *d* in Fig. 4f). When the LFA-1-ICAM-2 interaction is absent, the lever arm becomes longer (distance *d* in Fig. 4g) and the rolling velocity decreases. The distance '*d*' was indeed found to be significantly larger in LFA-1 deficient (*Itgal*$^{-/-}$) neutrophils compared to WT neutrophils (Fig. 4h; Supplementary note 4).

In conclusion, the discovery of slings provides a mechanism by which neutrophils rolling at high shear stress pave their own way for enhanced rolling. The patchy distribution of PSGL-1 along each sling provides a unique adhesive substrate once the cell rolls over the sling. As each PSGL-1 patch fails, a new patch is already lined up that now becomes load-bearing. This step-wise peeling makes slings even more efficient than tethers in slowing

down rolling neutrophils. Since slings accumulate over time, eventually, the rolling becomes very stable at high shear stresses[5]. Besides stabilizing rolling, slings are unique structures that also enable rolling neutrophils to present LFA-1 to its ligand ICAM-2 in *trans*. Taken together, catch bonds[22], long tethers[4], cell flattening[1,2,4] and now slings may explain why neutrophils can roll even at very high shear stress as observed in acute inflammation *in vivo*[1,3].

METHODS

Reagents

Recombinant murine P-selectin-Fc, E-selectin-Fc and ICAM-1-Fc were purchased from R&D Systems Inc. (Minneapolis, MN). Function blocking mAbs RB40.34 (rat IgG_1) against mouse P-selectin, TIB217 (rat IgG_{2a}) against mouse LFA-1, 4RA10 (rat IgG_1) against mouse PSGL-1, and 2.4G2 (rat IgG_{2b}) against mouse Fc-receptor were purified from hybridoma supernatant at the biomolecular facility of the University of Virginia, Charlottesville, VA. Function blocking Ab 3C4 (rat $IgG_{2a\kappa}$) against mouse ICAM-2 was purchased from BD Pharmingen (San Diego, CA). Non-blocking mAb 4RB12 (rat IgG_{2a}) against mouse PSGL-1 was a gift from Dietmar Vestweber, Max-Planck-Institute of Molecular Biomedicine, Münster, Germany. Alexa-Fluor-488 conjugated mAb 3C4 (rat $IgG_{2a\kappa}$) against mouse ICAM-2 and Alexa-Fluor-488 conjugated rat $IgG_{2a\kappa}$ isotype control Ab were purchased from BioLegend Inc. (San Diego, CA). Fluorescein-isothiocyanate (FITC) conjugated YN1 (rat $IgG_{2b\kappa}$) mAb against mouse ICAM-1 and FITC conjugated rat $IgG_{2b\kappa}$ isotype control Ab were purchased from eBioscience Inc. (San Diego, CA). DyLight-488 mAb labeling kit (cat# 53025) was purchased from Thermo Fisher Scientific Inc. (Rockford, IL). Alexa-Fluor-568 mAb labeling kit (cat# A-20184), Vybrant DiI (cat# V-22885) and DiO (cat# V-22886) were purchased from Molecular Probes, Inc. (Eugene, OR).

Mice

WT (C57BL/6J) mice (6–8 weeks old) were purchased from the Jackson Laboratory (Bar Harbor, ME). *Lyz2-EGFP* mice with the *EGFP* gene inserted into the lysozyme M (LysM, gene name, *Lyz2*) locus have been shown to express *EGFP* in the cytosol specifically in cells of myelomonocytic lineage (granulocytes and macrophages)[13]. *Lyz2-EGFP*, PSGL-1 deficient ($Selplg^{-/-}$)[23], and LFA-1 deficient ($Itgal^{-/-}$)[24] mice on C57BL/6J background were bred in house in a pathogen free animal facility at the La Jolla Institute for Allergy and Immunology (LIAI). Mice were handled according to the guidelines set by the Department of Laboratory Animal Care (DLAC) at LIAI and all surgical procedures were done as per the guidelines in the protocol approved by the Animal Care Committee of LIAI.

Microfluidic device

The assembly of microfluidic device used in this study and the coating of cover slips with recombinant murine P-selectin-Fc have been described previously[4,12]. P-selectin coating concentration of 2 and 1 μg/ml resulted in a P-selectin molecular density of ~20 and 10 molecules/μm^2, respectively, which is comparable to the P-selectin molecular density observed on endothelial cells[25,26]. In some experiments (Supplementary fig. 26), coverslips

were coated with a cocktail containing 2 μg/ml of recombinant murine P-selectin-Fc and 10 μg/ml of recombinant murine ICAM-1-Fc to create a substrate expressing both P-selectin and ICAM-1. Radioimmunoassay confirmed that the P-selectin molecular density was unaltered (20 molecules/μm^2) by the presence of ICAM-1 in the coating cocktail (data not shown).

Microfluidic perfusion assay

Neutrophils were isolated from the bone marrow of mice using immune-magnetic negative selection (EasySep mouse neutrophil enrichment kit; cat# 19709A; STEMCELL Technologies, Vancouver, BC) and stained with an intercalating membrane dye Vybrant DiO or DiI as described previously[12]. In some experiments, DiO or DiI stained neutrophils were additionally stained with Alexa-Fluor-568- or DyLight-488- conjugated 4RB12 or TIB217 mAbs. Stained (DiO or DiI) or unstained neutrophils (5–10 × 10^6 cells) were suspended in 200 μl Hanks Balanced Salt Solution without Ca^{2+} and Mg^{2+} (HBSS; GIBCO-Invitrogen, Carlsbad, CA) + 1% bovine serum albumin (BSA; cat# A7906, Sigma-Aldrich, St. Louis, MO), pH 7.4 and 2 μl of Fc-receptor blocking mAb 2.4G2 (0.5 mg/ml) was added to the cell suspension and cells were incubated for 10 min at room temperature. After 10 min, 4 μl of DyLight-488 or Alexa-Fluor-568-conjugated TIB217 mAb (0.62 mg/ml) or 2 μl of Alexa-Fluor-568- or DyLight-488- conjugated 4RB12 mAb (0.6 mg/ml) or both were added to the cell suspension and the cells were incubated for 30 min at room temperature. After 30 min, cells were washed twice in HBSS + 1% BSA and then, once in RPMI-1640 (GIBCO-Invitrogen) in a centrifuge (Sorvall RT, Thermo Scientific, Asheville, NC) at 300G (5 min, 22°C). Cells were finally suspended in RPMI-1640 + 10% mouse plasma at a concentration of 2.5 × 10^6 cells/ml and perfused through the microfluidic device at a wall shear stress of 6–10 dyn/cm^2. The microfluidic device was placed on the stage of TIRF microscope and images were recorded using qDF[4] or DqDF[12] scheme. In a different set of experiments (Fig. 4d and Supplementary fig. 26), bone marrow neutrophils from WT or *Itgal*$^{-/-}$ mice (2.5 × 10^6 cells/ml in RPMI + 10% mouse plasma) either untreated or blocked with 30 μg/ml (in cell suspension) of function blocking TIB217 or 3C4 mAb were perfused through the microfluidic device at a wall shear stress of 10 dyn/cm^2. The data shown in Figure 4e and Supplementary figure 27–28 was generated by incubating bone marrow neutrophils from WT mice with 2 μl of 2.4G2 mAb (0.5 mg/ml) in 200 μl of HBSS + 1% BSA at room temperature for 10 minutes. After 10 minutes, 4 μl of Alexa-Fluor-568-conjugated TIB217 mAb (0.62 mg/ml) together with 4 μl of Alexa-Fluor-488-conjugated 3C4 mAb (0.5 mg/ml) or rat $IgG_{2a\kappa}$ isotype control Ab (0.5 mg/ml) was added and cells were incubated for 30 minutes at room temperature. Finally, cells were washed twice with HBSS + 1% BSA and once with RPMI-1640 in a centrifuge at 300G (5 min, 22° C) and suspended in RPMI-1640 + 10% mouse plasma at a concentration of 2.5 × 10^6 cells/ml. Cells were perfused through the microfluidic device at a wall shear stress of 10 dyn/cm^2 and images were recorded using DqDF. Incubation of neutrophils with function blocking anti-mouse PSGL-1 (4RA10) mAb abolished all rolling on P-selectin.

Auto-perfused microfluidic perfusion assay

The auto-perfused microfluidic perfusion assay has been described previously[4] in detail.

Isolation of naïve CD4T cells and differentiation into Th1 cells

Naïve CD4T cells were isolated from the spleen of WT mice using EasySep-mouse-CD4T-cell enrichment kit (STEMCELL Technologies) and *in vitro* differentiated into Th1 cells as described elsewhere[27]. Cells were stained with 1.5 μM DiI and suspended in RPMI-1640 + 10% mouse plasma at a concentration of 2.5×10^6 cells/ml. Incubation of Th1 cells with function blocking anti-mouse PSGL-1 (4RA10) mAb abolished all rolling on P-selectin.

Expression of ICAM-1 and ICAM-2 on mouse neutrophils

Expression of ICAM-1 and ICAM-2 on mouse blood and bone marrow neutrophils were measured using flow cytometry. Blood and bone marrow neutrophils from WT mice were stained with FITC-conjugated YN1 mAb against mouse ICAM-1 or Alexa-Fluor-488 conjugated 3C4 mAb against mouse ICAM-2 or respective isotype control Abs and flow cytometric analysis was done using BD FACSCanto II flow cytometer, BD Biosciences (San Jose, CA).

qDF and DqDF microscopy

The qDF and DqDF setups and the theory of qDF have been described previously in detail[4,12]. The set up consisted of an IX71 inverted TIRF research microscope (Olympus America Inc., Center Valley, PA) with a 100x NA 1.45 Plan-Apochromatic oil immersion TIRFM objective and 30 mW blue (λ = 488nm) and 20 mW yellow-green (λ = 561 nm) diode-pumped-solid-state lasers (CVI Melles Griot, Carlsbad, CA) as TIRF excitation light sources. Images were captured at a rate of 2 to 8 frames/s using DV2 (PHOTOMETRICS, Tucson, AZ) DualView video coupler and a 16 bit digital CCD camera (HAMAMATSU C10600-10B ORCA-R^2). The laser shutters and camera were controlled with the SlideBook5.0 software (Intelligent Imaging Innovations Inc., Santa Monica, CA) which has built-in features for image analysis. The absorption and emission peaks of the fluorochromes used in this study were, respectively, 488 and 507 nm for *EGFP*, 484 and 501 nm for DiO, 549 and 565 nm for DiI, 493 and 518 nm for DyLight-488, 579 and 603 nm for Alexa-Fluor-568, and 495 and 515 nm for Alex-Fluor-488. A TIRF incidence angle of θ = 70° was used for both lasers in all qDF and DqDF experiments.

Image processing of qDF images

qDF and DqDF images were saturated to reveal slings and tether anchorage points as described previously[4]. Briefly, the scale of the intensity histogram of a qDF image was flattened by fixing the maxima close to the minima to reveal fine structures like slings and tether anchor points (Fig. 1a–b, 2d, 3a–c). Saturation of images causes cells to appear bigger than their actual size.

Creation of 3D-reconstructions and 2D-color maps

Raw DiO or DiI qDF images were used to create 3D-reconstructions (Fig. 1c–d, 4c and Supplementary fig. 6b and 7b) or 2D-color maps (Supplementary fig. 14a) of the footprints as described previously[4,12].

Scanning electron microscopy

Neutrophils from WT mice rolling on P-selectin (20 molecules/μm^2) in a microfluidic device at a shear stress of 10 dyn/cm^2 were fixed by perfusing a cocktail containing 2% paraformaldehyde, 2.5% glutaraldehyde, 1 mM $CaCl_2$, and 0.1 M sodium cacodylate buffer (pH 7.4) in distilled water. Fixed cells were visualized using a scanning electron microscope (S-450; Hitachi, Tokyo, Japan) as described elsewhere[28]. The diameter of the sling and neutrophil were estimated from electron micrographs using NIH-Image J (National Institutes of Health, Bethesda, MD). The reported values are corrected based on 30% shrinkage as determined by the cell diameter measurements before and after fixation.

Epifluorescence intravital microscopy

Surgical-trauma-induced rolling of neutrophils in the cremaster venules of mice is a model of acute inflammation[29] and the rolling within 60 min following surgery is primarily mediated by P-selectin on the endothelium binding to PSGL-1 on neutrophils[30,31]. Each WT mouse was anesthetized, its trachea was intubated, right carotid artery was cannulated, and the cremaster muscle was prepared for intravital microscopy as described previously[29]. To increase contrast, neutrophil surfaces were labeled *in vivo* with DyLight-488-conjugated TIB217 mAb (green) against mouse LFA-1, which is highly expressed on the cell surface including slings (Fig. 4c). Immediately before microscopic observations, 25 μg of DyLight-488-conjugated TIB217 mAb was injected via the catheter connected to the right carotid artery. A glass cover slip (No.1; 1 cm × 1 cm) was placed over the moistened cremaster muscle and epifluorescence observations were recorded using a 100x NA = 1.45 Plan-Apochromatic oil immersion objective on an Olympus BX61 upright microscope. Images were recorded using a 16 bit digital CCD camera (HAMAMATSU C10600-10B ORCA-R^2) which was connected to a PC (Dell Precision T3400; Intel Core 2 Duo CPU-3.16 GHz; 3.25 GB RAM) through an IEEE1394b interface. Images were recorded at the rate of 7–16 frames/s and 2×2 binning as well as contrast enhancement (Fig. 1h–m, Supplementary fig. 1 and Supplementary movies 4 and 5) was done post-acquisition using SlideBook5.0.

Estimation of tether and sling force

At any of the steps 3–5 during the step-wise peeling of a sling (Fig. 3f), the sling acts just like a tether by balancing not only the forward force but also the bond torque acting on the rolling cell. Thus, a sling was treated as a tether in estimating its contribution in sharing of hydrodynamic load (Fig. 2f). Figure 2f shows the force F acting on a tether or sling starting from the time point when F exceeds 31 pN for the first time and before the tether or the load-bearing patch on the sling detaches from the substrate (t = 0 s; step 6 in Fig. 3f). The parameters used for force calculation were the cell radius[32] r_c = 4 μm, membrane curvature modulus[11] k_c = 0.2 pN μm, membrane interfacial drag coefficient[8] d_{int} = 600 pN s/μm^3, tether threshold force[8] F_{th} = 31 pN, and average tether anchorage point to-substrate distance of 135 nm (based on qDF measurements). The variables used for the calculation of force, *viz*. cell translational velocity V_{tr}, cell-substrate separation distance, and the horizontal distance between the tether anchorage point and the projection of the cell center on the substrate (the anchor-cell-center projection line) were measured experimentally using qDF. However, the exact location of the base of a tethered microvillus cannot be determined

precisely by qDF measurements. For simplicity, we assumed that the projection of the tether's microvillus base is on the anchor-cell-center projection line when the tether anchorage point starts to be seen (changing reasonably the location of the microvillus base yielded similar results). The tether extension rate dL/dt, where L is the tether extension, was calculated geometrically assuming that the cell rotational velocity[33], $V_{rot} = 0.97V_{tr}$. The tether force F was calculated numerically from the formula $dL/dt = [F^3 - F(F_{th})^2]/[16\pi^3(k_c)^2 d_{int} \ln(r_c F/2\pi k_c)]$ assuming the tether to be a nonlinearly decaying spring viscoelastic (NLDs-viscoelastic)[8,34].

Fraction of cell forward force and torque balanced by slings and tethers

Based on the findings of the current and previous study[4], a plausible scenario was considered where a rolling neutrophil has two peeling slings, each with the inflection point or the loaded patch at a distance of 10 μm from the cell center (distance shown by double headed arrow in step 3 of Fig. 3f) and two tethers with anchorage points at a distance of 10 μm from the cell center (distance shown by double headed arrow in step 1 of Fig. 3f). The total forward force and torque acting on the rolling cell were estimated for wall shear stresses of 6 and 8 dyn/cm^2 using Goldman's theory[35–38], assuming that the cell is spherical of radius $r_c = 3.75$ μm, the translational velocity $V_{tr} = 2.4$ μm/s (based on qDF data), and the rotational velocity[33] is $0.97V_{tr}$. The fractions of forward force and torque balanced by two slings and two tethers are shown in Figure 2g and Supplementary figure 3. The values were calculated based on geometry of the tethers or slings having projection lengths of 10 μm and force loads of 60 pN (average force shown by red line in Fig. 2f). The fractions were also calculated for $r_c = 4$ μm (data not shown).

Statistical analysis

The pairs of means for the data sets in Figures 3d, 3e, 4h and Supplementary figures 14 and 15 were compared, each separately, using student *t*-tests with equal variances. The pairs of means for the data sets in Figures 2c, 4d and Supplementary figure 26 were compared using Bonferroni *t*-tests[39] where the significance levels for individual pairs were adjusted based on the number of data entries and number of comparison groups to secure the overall significance level of 0.05.

Supplementary Material

Refer to Web version on PubMed Central for supplementary material.

Acknowledgments

The authors thank Arturo Zychlinsky, Max Planck Institute, Berlin for comments and reading the manuscript. This study was supported by the NCRP-Scientist Development Grant 11SDG7340005 from the American Heart Association (P.S.), WSA postdoctoral fellowship 10POST4160142-01 from American Heart Association (E.K.K.) and NIH EB 02185 (K.L.).

References

1. Firrell JC, Lipowsky HH. Leukocyte margination and deformation in mesenteric venules of rat. Am J Physiol Heart Circ Physiol. 1989; 256:H1667–1674.

2. Sundd P, Pospieszalska MK, Cheung LS, Konstantopoulos K, Ley K. Biomechanics of leukocyte rolling. Biorheology. 2011; 48:1–35. [PubMed: 21515934]

3. Damiano ER, Westheider J, Tozeren A, Ley K. Variation in the velocity, deformation, and adhesion energy density of leukocytes rolling within venules. Circ Res. 1996; 79:1122–1130. [PubMed: 8943950]

4. Sundd P, et al. Quantitative dynamic footprinting microscopy reveals mechanisms of neutrophil rolling. Nat Methods. 2010; 7:821–824. [PubMed: 20871617]

5. Ramachandran V, Williams M, Yago T, Schmidtke DW, McEver RP. Dynamic alterations of membrane tethers stabilize leukocyte rolling on P-selectin. Proceedings of the National Academy of Sciences USA. 2004; 101:13519–13524.

6. Schmidtke DW, Diamond SL. Direct observation of membrane tethers formed during neutrophil attachment to platelets or P-selectin under physiological flow. Journal of Cell Biology. 2000; 149:719–729. [PubMed: 10791984]

7. Shao, JY. Biomechanics of leukocyte and endothelial cell surface in *Leukocyte adhesion*. Ley, Klaus, editor. Academic press; San Diego: 2009. p. 25-45.

8. Pospieszalska MK, Lasiecka I, Ley K. Cell protrusions and tethers: a unified approach. Biophys J. 2011; 100:1697–1707. [PubMed: 21463583]

9. Hocdé SA, Hyrien O, Waugh RE. Cell Adhesion Molecule Distribution Relative to Neutrophil Surface Topography Assessed by TIRFM. Biophysical Journal. 2009; 97:379–387. [PubMed: 19580776]

10. Moore KL, et al. P-selectin glycoprotein ligand-1 mediates rolling of human neutrophils on P-selectin. Journal of Cell Biology. 1995; 128:661–671. [PubMed: 7532174]

11. Waugh, RE. Membrane tethers in *Leukocyte adhesion*. Academic press; San Diego: 2009. p. 3-24.

12. Sundd P, et al. Live cell imaging of paxillin in rolling neutrophils by dual-color quantitative dynamic footprinting. Microcirculation. 2011; 18:361–372. [PubMed: 21418380]

13. Faust N, Varas F, Kelly LM, Heck S, Graf T. Insertion of enhanced green fluorescent protein into the lysozyme gene creates mice with green fluorescent granulocytes and macrophages. Blood. 2000; 96:719–726. [PubMed: 10887140]

14. Pendl GG, et al. Immature mouse dendritic cells enter inflamed tissue, a process that requires E- and P-selectin, but not P-selectin glycoprotein ligand 1. Blood. 2002; 99:946–956. [PubMed: 11806998]

15. Springer TA. Traffic signals for lymphocyte recirculation and leukocyte emigration: the multistep paradigm. Cell. 1994; 76:301–314. [PubMed: 7507411]

16. Xu H, et al. Characterization of murine intercellular adhesion molecule-2. Journal of Immunology. 1996; 156:4909–4914.

17. Zarbock A, Lowell CA, Ley K. Spleen tyrosine kinase Syk is necessary for E-selectin-induced alpha(L)beta(2) integrin-mediated rolling on intercellular adhesion molecule-1. Immunity. 2007; 26:773–783. [PubMed: 17543554]

18. Lawrence MB, Springer TA. Leukocytes roll on a selectin at physiological flow rates: distinction from and prerequisite for adhesion through integrins. Cell. 1991; 65:859–874. [PubMed: 1710173]

19. Kuwano Y, Spelten O, Zhang H, Ley K, Zarbock A. Rolling on E- or P-selectin induces the extended but not high-affinity conformation of LFA-1 in neutrophils. Blood. 2010; 116:617–624. [PubMed: 20445017]

20. Woodfin A, et al. The junctional adhesion molecule JAM-C regulates polarized transendothelial migration of neutrophils in vivo. Nature Immunology. 2011; 12:761–769. [PubMed: 21706006]

21. Huang MT, et al. ICAM-2 mediates neutrophil transmigration in vivo: evidence for stimulus specificity and a role in PECAM-1-independent transmigration. Blood. 2006; 107:4721–4727. [PubMed: 16469869]

22. Marshall BT, et al. Direct observation of catch bonds involving cell-adhesion molecules. Nature. 2003; 423:190–193. [PubMed: 12736689]

23. Xia L, et al. P-selectin glycoprotein ligand-1-deficient mice have impaired leukocyte tethering to E-selectin under flow. Journal of Clinical Investigation. 2002; 109:939–950. [PubMed: 11927621]

24. Ding ZM, et al. Relative contribution of LFA-1 and Mac-1 to neutrophil adhesion and migration. J Immunol. 1999; 163:5029–5038. [PubMed: 10528208]
25. Hattori R, Hamilton K, Fugate R, McEver R, Sims P. Stimulated secretion of endothelial von Willebrand factor is accompanied by rapid redistribution to the cell surface of the intracellular granule membrane protein GMP-140. J Biol Chem. 1989; 264:7768–7771. [PubMed: 2470733]
26. Doyle EL, et al. CD63 is an essential cofactor to leukocyte recruitment by endothelial P-selectin. Blood. 2011; 118:4265–4273. [PubMed: 21803846]
27. Atarashi K, Hirata T, Matsumoto M, Kanemitsu N, Miyasaka M. Rolling of Th1 Cells via P-Selectin Glycoprotein Ligand-1 Stimulates LFA-1-Mediated Cell Binding to ICAM-1. J Immunol. 2005; 174:1424–1432. [PubMed: 15661900]
28. Tojo A, et al. Nitric oxide generated by nNOS in the macula densa regulates the afferent arteriolar diameter in rat kidney. Med Electron Microsc. 2004; 37:236–241. [PubMed: 15614448]
29. Ley K, et al. Sequential contribution of L- and P-selectin to leukocyte rolling in vivo. J Exp Med. 1995; 181:669–675. [PubMed: 7530761]
30. Kunkel EJ, et al. Absence of trauma-induced leukocyte rolling in mice deficient in both P-selectin and intercellular adhesion molecule 1. Journal of Experimental Medicine. 1996; 183:57–65. [PubMed: 8551244]
31. Sperandio M, et al. Severe impairment of leukocyte rolling in venules of core 2 glucosaminyltransferase-deficient mice. Blood. 2001; 97:3812–3819. [PubMed: 11389021]
32. Schmid-Schonbein GW. Leukocyte biophysics. An invited review. Cell Biophys. 1990; 17:107–135. [PubMed: 1705479]
33. Pospieszalska, MK.; Ley, K. Modeling leukocyte rolling in *Leukocyte adhesion*. Ley, Klaus, editor. Vol. 64. Elsevier; San Diego: 2009. p. 221-296.
34. Brochard-Wyart F, Borghi N, Cuvelier D, Nassoy P. Hydrodynamic narrowing of tubes extruded from cells. Proc Natl Acad Sci U S A. 2006; 103:7660–7663. [PubMed: 16679410]
35. Goldman AJ, Cox RG, Brenner H. Slow viscous motion of a sphere parallel to a plane wall. II. Couette flow. Chemical Engineering Science. 1967; 22:653–660.
36. Pospieszalska MK, Zarbock A, Pickard JE, Ley K. Event-tracking model of adhesion identifies load-bearing bonds in rolling leukocytes. Microcirculation. 2009; 16:115–130. [PubMed: 19023690]
37. Krasik EF, Hammer DA. A Semianalytic Model of Leukocyte Rolling. Biophys J. 2004; 87:2919–2930. [PubMed: 15315955]
38. Goldman AJ, Cox RG, Brenner H. Slow viscous motion of a sphere parallel to a plane wall I. Motion through a quiescent fluid. Chemical Engineering Science. 1967; 22:637–652.
39. Wilcox, RR. New statistical procedures for the social sciences: Modern solutions to basic problems. Lawrence Erlbaum Associates, Inc., Publishers; Hillsdale, NJ: 1987.

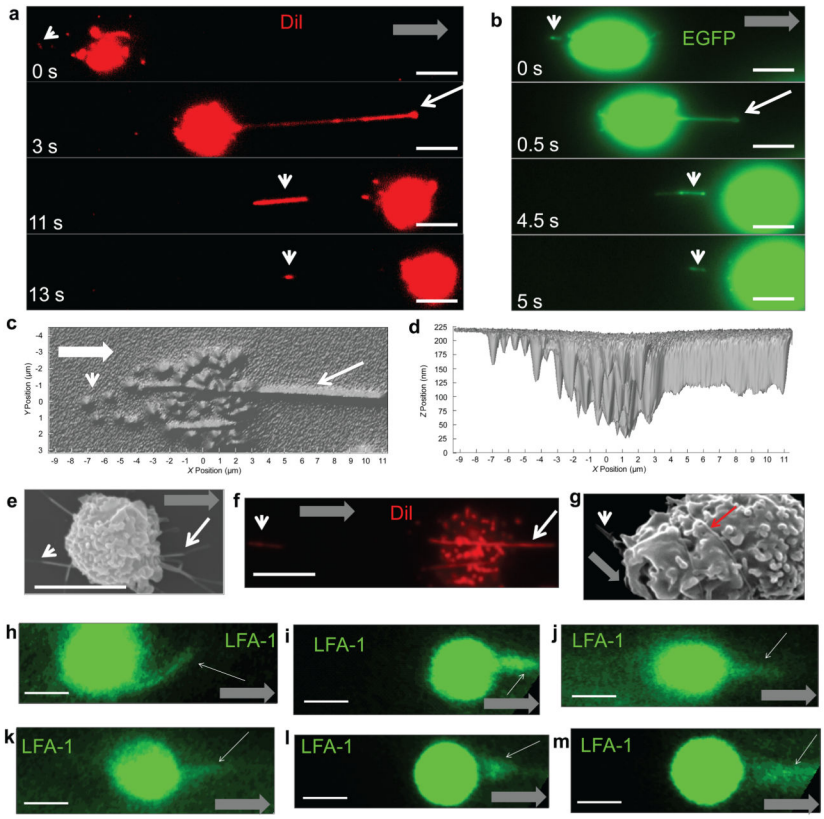

Figure 1. Rolling neutrophils form slings

Processed qDF images of (**a**) a DiI-stained isolated neutrophil and (**b**) an *EGFP* neutrophil (in whole blood) rolling on P-selectin in a microfluidic device. A tether (anchor point marked with white arrowhead at t = 0 s) swings around to the front of the cell as a 'sling' (white arrow) at t = 3 s (**a**) and 0.5 s (**b**). (**c–d**) 3D-reconstruction of the footprint of a rolling neutrophil. x–y plane (**c**) and x–z plane (**d**). (**e**) SEM of a rolling neutrophil showing tethers and slings. (**f**) Unprocessed qDF image of a DiI-stained neutrophil rolling on P-selectin reveals wrapping of slings. (**g**) SEM showing sling (red arrow) wrapped around a rolling neutrophil. (**h–m**) Epifluorescence intravital microscopic images demonstrating sling formation by six different leukocytes. P-selectin (a–g) 20 molecules/μm^2. Shear stress 10 dyn/cm^2 (a, c–g), 8 dyn/cm^2 (b). Tether anchor points, arrowheads; Sling, thin arrow; Rolling direction, thick arrow. Scale bars 5 μm.

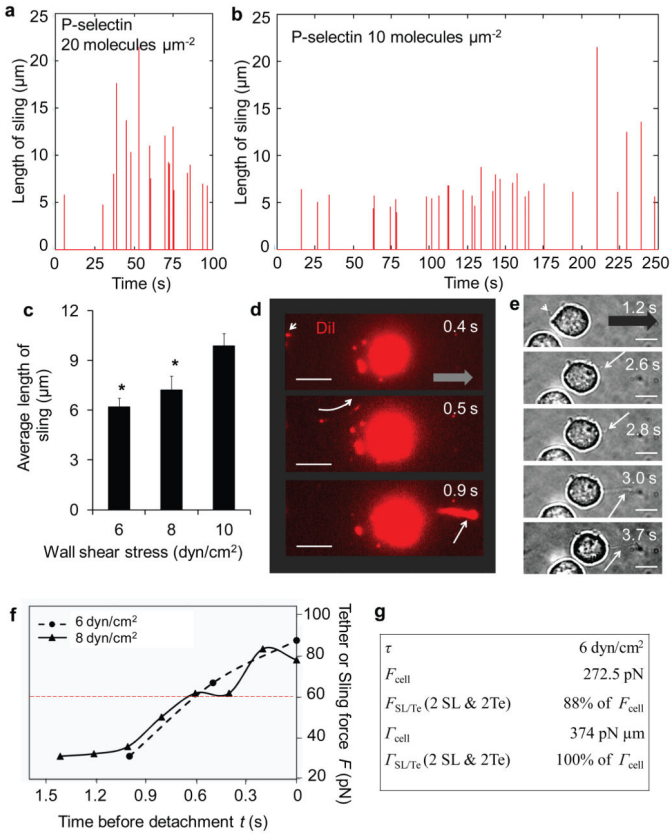

Figure 2. Sling formation, length and force

(**a–b**) Length of slings formed by a single neutrophil rolling on (**a**) 20 and (**b**) 10 P-selectin molecules/μm^2 in a microfluidic device. (**c**) Average length of slings as a function of shear stress. Error bars s.e.m. '*' $p < 0.05$ relative to 10 dyn/cm^2; n = 34, 47, and 64 for 6, 8, and 10 dyn/cm^2, respectively. (**d**) A tether (arrowhead at 0.4 s) swings to the front as a sling (white arrow at 0.9 s). qDF images processed. (**e**) A tether (arrowhead at 1.2 s) swings to the front as a sling (white arrow at 3 s). DIC images. Shear stress 10 dyn/cm^2. P-selectin 20 molecules/μm^2. Scale bars 5 μm. Rolling direction, thick arrow. (**f**) Sling or tether force F before detachment from the substrate. Solid curve, 8 dyn/cm^2; dashed curve, 6 dyn/cm^2; solid symbols, qDF data. (**g**) Fraction of the forward cell force and torque balanced by 2 slings and 2 tethers. τ, shear stress; F_{cell}, total forward force; $F_{SL/Te}$, forward force balanced by 2 slings and 2 tethers; Γ_{cell}, total torque; $\Gamma_{SL/Te}$, torque balanced by 2 slings and 2 tethers. Data in a–f representative of five independent experiments.

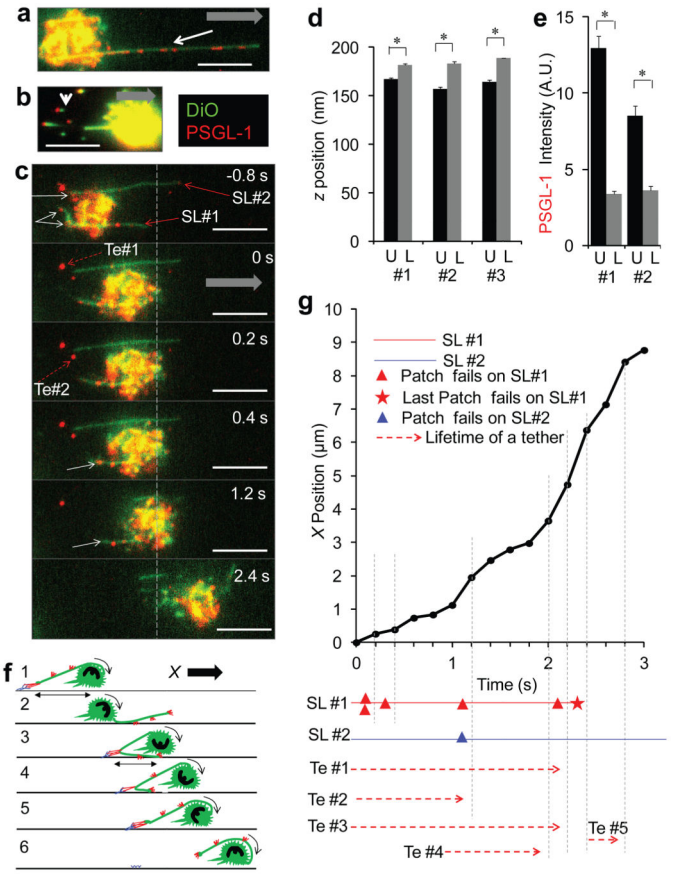

Figure 3. Neutrophil rolling is stabilized by step-wise peeling of slings

(**a**) PSGL-1 expressed in patches (red spots) on the sling (green; white arrow). (**b**) PSGL-1 (red spots) concentrated in the tether anchorage points (green; white arrowhead). (**c**) Two slings and anchorage points of two tethers denoted as 'SL#1 and 2 (red solid arrow)' and 'Te#1 and 2 (red dashed arrow)', respectively. PSGL-1 patches at the inflection point of SL#1 and 2 visible as red spots (solid white arrow) at −0.8 s. As the cell rolls forward the SL#1 and 2 become load-bearing at 0 s which is evident by the apparent loss of PSGL-1 staining (red) in these patches. The two load-bearing patches on SL#1 fail between 0 and 0.2 s and the next two downstream patches on SL#1 become load-bearing (red fluorescence in these patches reduced at 0.2 s). The last PSGL-1 patch on the SL#1 fails between 2.2 and 2.4 s. Refer Supplementary fig. 13 for details. (**d**) The *z*-distance of the sling membrane from the cover slip in three different PSGL-1 patches. (**e**) PSGL-1 fluorescence intensity for two PSGL-1 patches. U, unloaded. L, loaded. '*' $p < 0.05$. Error bars s.e.m. (**f**) Schematic of step-wise peeling mechanism. Cell (green), PSGL-1 (red) and P-selectin (blue). (**g**) Position of the cell shown in c plotted as a function of time. Closed circles, cell position; red and blue solid lines, SL#1 and 2, respectively; red and blue closed triangles, failure of individual patches on SL#1 and 2, respectively; red-five-point-star, failure of last patch on SL#1; red-dashed horizontal arrow, lifetime of a tether. Shear stress 10 dyn/cm^2. P-selectin 20 molecules/μm^2. Scale bars 5 μm. Rolling direction, thick arrows. DqDF images (**a–c**) were processed. Data representative of six independent experiments.

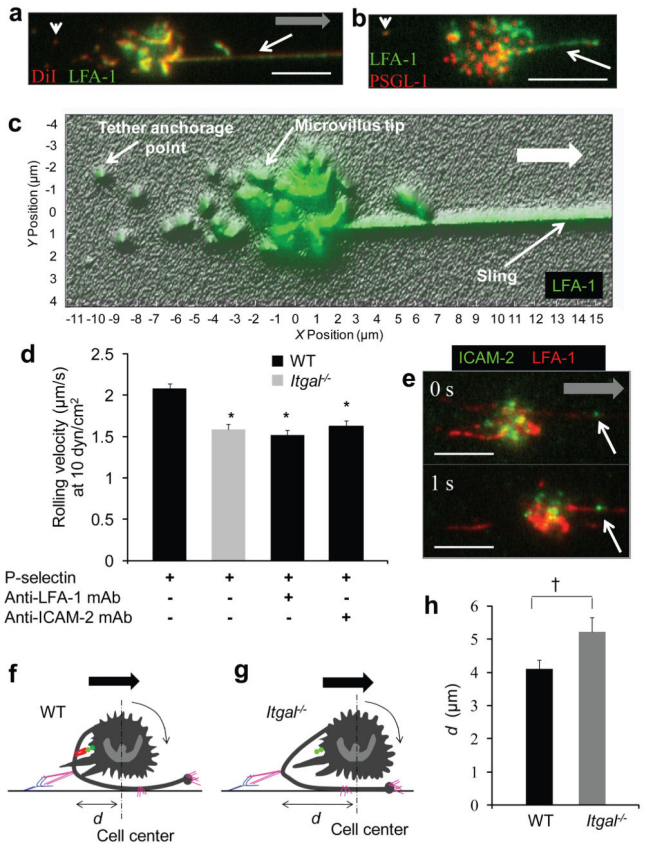

Figure 4. Slings enable LFA-1-ICAM-2 interactions in *trans*

Neutrophils stained with (a) DiI (red) and DyLight-488-TIB217 mAb (green) or (**b**) DyLight-488-TIB217 mAb (green) and Alexa-Fluor-568-4RB12 mAb (red) were allowed to roll on P-selectin and footprints visualized using DqDF. (**c**) The DiI footprint (red; Supplementary fig. 20) analyzed to generate a 3D-reconstruction and the LFA-1 image (green; Supplementary fig. 20) overlaid to reveal distribution of LFA-1 (green) on sling, tether anchorage points, and microvilli (grey hills) vs. cell surface (valleys). (**d**) Mean rolling velocity of neutrophils on P-selectin. WT (black; $n = 159$), *Itgal*$^{-/-}$ (grey; $n = 173$), WT blocked with anti-LFA-1 mAb (black; $n = 142$), and WT blocked with anti-ICAM-2 mAb (black; $n = 98$). '*' $p < 0.01$ relative to WT without blocking. (**e**) DqDF images of a rolling neutrophil show distribution of LFA-1 (red) and ICAM-2 (green). (**f–g**) Schematics showing the mechanism of LFA-1-ICAM-2 interactions in *trans*. *d*, distance of the rearmost load-bearing patch at the inflection point of the sling from the cell center; LFA-1 (red); ICAM-2 (green); PSGL-1 (violet); P-selectin (blue). (**h**) Mean '*d*' plotted for WT ($n = 56$) and *Itgal*$^{-/-}$ ($n = 53$) neutrophils. '†' $p < 0.05$. Shear stress 10 dyn/cm^2. P-selectin 20 molecules/μm^2. Scale bars 5 μm. Tether anchorage points, white arrowheads; Slings, white arrows. Rolling direction, thick arrow. Error bars s.e.m. Data representative of five (**a–c**), four (**d**), and three (**e, h**) experiments.